



# Magnetic properties of transition-metal-doped a-Fe<sub>90</sub>Zr<sub>10</sub>

D.H. Ryan<sup>a,\*</sup>, J.M. Cadogan<sup>b</sup>

<sup>a</sup>Physics Department, McGill University, 3600 University Street, Montreal, Quebec H3A 2T8, Canada

<sup>b</sup>School of Physics, The University of New South Wales, Sydney, NSW 2052, Australia

Received 19 April 1999; received in revised form 7 December 1999

## Abstract

The magnetic properties of transition metal-doped a-Fe<sub>90</sub>Zr<sub>10</sub> have been studied by magnetisation, susceptibility and Mössbauer spectroscopy. The results of our survey confirm that Ru is more than twice as effective at destroying the magnetic order than any other dopant. Comparison of changes in moment and average hyperfine field allow us to deduce a conversion factor of  $14.3 \pm 0.8 \text{ T}/\mu_{\text{B}}$  for <sup>57</sup>Fe. © 2000 Elsevier Science B.V. All rights reserved.

PACS: 76.80.+y; 75.50.Bb; 75.50.Lk; 75.50.Kj

Keywords: Mössbauer; Magnetic properties; Metallic glasses; Spin-glasses

## 1. Introduction

The amorphous Fe–Zr system spans the full range of correlated electron behaviour in metals, from superconductivity through spin-fluctuations and ferromagnetism, and ultimately into spin-glasses [1–3]. As a result, it provides an ideal matrix in which to investigate the effects of doping on magnetic properties. In the binary system a-Fe<sub>x</sub>Zr<sub>100-x</sub>, both  $T_c$  and the magnetisation fall rapidly for  $x > 90$ . We have previously demonstrated that this is due to the effects of exchange frustration [4] and that this behaviour is fully consistent with the predictions of numerical simulations [5].

Exchange frustration in the a-Fe–Zr system arises through competing direct exchange interactions ( $\mathcal{J}$ ). Positive and negative  $\mathcal{J}$ 's are present as a result of a fortuitous sign change in the interaction at a distance corresponding roughly to iron's metallic diameter. The detailed behaviour of  $\mathcal{J}$  is quite complex and depends both on bond-length and on the mean electron density in the alloy [6,7]. Dopants can therefore modify the exchange distribution in two ways. Where there is a significant size mismatch or a large volume change associated with the dopant (e.g. with hydrogen) the dopant can simply increase the average bond-length and eliminate the short contacts that contribute to the frustration [3,8]. Where the size difference is small (e.g. most transition metals) changes in the average electron density can move the  $+\mathcal{J} \rightarrow -\mathcal{J}$  crossover distance, without affecting the actual distribution of bond-lengths, and so modify the distribution of exchange interactions indirectly. In general, both effects will be present to some degree.

\* Corresponding author. Tel.: +1-514-398-6534; fax: +1-514-398-6526.

E-mail address: dominic@physics.mcgill.ca (D.H. Ryan).

While no systematic studies have been described, the changes in the magnetic properties of iron-rich a-Fe–Zr caused by various 3-d transition metals have been widely reported, and some representative data can be found for: Cr [9], Mn [10], Co [11,12] and Ni [13,14]. Of the 4-d series, only Ru has drawn significant attention [15–18]. We report here a systematic study of the effects of all possible d-transition metal dopants on the magnetic properties of a-Fe<sub>90-x</sub>TM<sub>x</sub>Zr<sub>10</sub>, i.e. close to the ferromagnet–spin-glass crossover. While some of the systems studied will accommodate substantial doping levels (e.g. Co and Ni can be prepared all of the way to  $x = 90$  [19–21]) the maximum levels used here were limited to  $x = 10$ . In many cases, the glasses were not stable and even these doping levels could not be attained.

## 2. Experimental methods

Ribbons of a-Fe<sub>90-x</sub>TM<sub>x</sub>Zr<sub>10</sub> were prepared by arc-melting appropriate amounts of the pure elements under Ti-gettered argon, followed by melt-spinning in 40 kPa helium with a tangential wheel speed of 55 m/s.

The following transition metals were successfully doped into the system:

3-d V → Cu.

No exceptions.

4-d Zr → Pd.

Zr-Data taken from earlier work [3,4]

Nb-no usable material produced

Tc-not practical

Ag-high vapour pressure and immiscibility with Fe made samples highly suspect.

5-d W → Au.

No exceptions.

The materials produced ranged from good-quality metre-length amorphous ribbons to crystalline dust. The primary contaminant in poorly quenched iron-rich a-Fe–Zr alloys is  $\alpha$ -Fe, which is easily detected. In most cases, the  $T_c$  of the glassy alloy was below room temperature and so simple mechanical and magnetic tests were sufficient to reject poor samples (brittle or highly magnetic materials were generally partially crystalline). The remaining materials were checked for crystalline contami-

nants (primarily  $\alpha$ -Fe) by Cu K <sub>$\alpha$</sub>  X-ray diffraction on a conventional automated powder diffractometer, and room temperature <sup>57</sup>Fe Mössbauer spectroscopy. The magnetic ordering temperatures were determined using AC susceptibility (for  $T_c < 320$  K) or thermogravimetric analysis (TGA) in a small field gradient (for  $T_c > 320$  K). In both cases, the presence of a significant background signal above  $T_c$  was taken as an indication of a crystalline contaminant. These samples were also rejected.

Where the yield of quality ribbon was high enough, room temperature and 12 K Mössbauer spectra were obtained on a conventional constant-acceleration spectrometer using a 1 GBq <sup>57</sup>CoRh source. Low-temperature spectra were obtained using a vibration-isolated closed-cycle fridge. The paramagnetic spectra were fitted assuming a Gaussian distribution of quadrupole splittings ( $\Delta$ ), with a linear correlation between  $\Delta$  and the isomer shift ( $\delta$ ) included to account for the observed asymmetry in the spectra. The magnetic spectra were fitted using Window's method [22]. The room temperature values for  $\delta$  and  $\Delta$ , along with the 12 K values for  $\langle B_{hf} \rangle$  were taken directly from fits to the Mössbauer data. When substantial amounts of iron are replaced, there may, in principle, be changes in the atomic packing in the glass which can be detected through the quadrupole splitting [23]. However, here  $\Delta$  was found to be essentially constant at  $0.34 \pm 0.01$  mm/s and exhibited no systematic variation with composition. We take this as evidence for a constant glass structure at the doping levels used in this study.

Smaller samples were needed for the magnetic measurements, and even when the yield was poor, it was often possible to select sufficient material for susceptibility and magnetisation studies although Mössbauer measurements were not possible.  $T_c$  was defined by the extrapolation of the point of maximum slope on a plot of  $\chi$  versus  $T$  to zero signal. Since many of the samples are highly frustrated and so not collinear ferromagnets, their magnetisation did not saturate in 9 T and the curves exhibited a substantial high-field slope. We therefore took the magnetisation at 5 K ( $\sigma_0$ ) from a linear extrapolation of the high-field (typically  $B_0 \geq 5$  T) region of the magnetisation curve to zero field.

### 3. Results and discussion

The composition dependence of the isomer shift (Fig. 1) shows a particularly simple form. Elements to the left of Fe decrease  $\delta$ , while those to the right cause an increase. Essentially similar results have been reported for dilute impurities in crystalline iron [24,25]. This trend reflects a tendency for the early transition metals to transfer electrons to the Fe, while the later elements have a stronger tendency to remove electrons. Those on the left also have very similar effects with little variation between rows of the periodic table, whereas there are increasingly strong row-dependent effects evident to the right of Fe. As noted above, we observed no systematic composition dependence in the quadrupole splitting, and interpret this as a reflection of an essentially constant glass structure. Furthermore, as the observed changes in  $\delta$  are dominated by s-electron transfer [26] no direct magnetic consequences are anticipated. The isomer shift therefore serves here primarily as an independent indicator that the dopants are indeed alloying into the glass.

Despite the simple form of the electron transfer behaviour and the unchanging structure of the glass, the magnetic ordering temperatures exhibit a more complex dependence on dopant (Fig. 2). Most values of  $dT_c/dx$  shown in Fig. 2 are derived from linear fits to  $T_c$  versus  $x$ . In some cases, the composition dependence was nonlinear (e.g. both

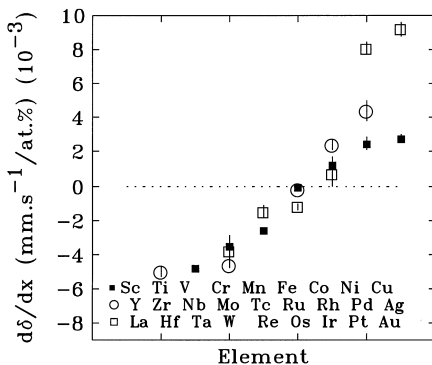


Fig. 1. The rate of change of the isomer shift,  $\delta$ , at room temperature for  $a\text{-Fe}_{90-x}\text{TM}_x\text{Zr}_{10}$  alloys, where TM is a 3d, 4d or 5d transition metal.

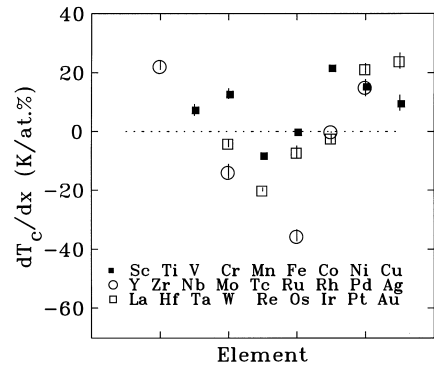


Fig. 2. The rate of change of the magnetic ordering temperature,  $T_c$ , for  $a\text{-Fe}_{90-x}\text{TM}_x\text{Zr}_{10}$  alloys, where TM is a 3d, 4d or 5d transition metal.

Cr and Au cause  $T_c$  to go through a clear maximum at  $x \sim 5$  and  $\sim 9$  at% respectively) so a quadratic term was included and the initial slope is plotted in Fig. 2. The basic picture is relatively simple: a broad minimum is located between Mn and Fe, with elements both to the left and to the right leading to an increase in  $T_c$ . This pattern is quite different from that seen for  $\delta$  in Fig. 1 indicating that electron transfer, as expected, does not control  $T_c$ . Of the 18 elements surveyed, only seven lead to a reduction in  $T_c$ . Ru causes the most rapid reduction in  $T_c$  by far, while Zr, Co, Ni and Au all lead to quite similar increases. Since both magnetic and nonmagnetic dopants have comparable effects, it is clear that dopant moments are not the dominant factor in determining  $T_c$  shifts. Finally, dopant size does not correlate well with the observed change in  $T_c$ . For example, Re and Pt differ in size by only  $\sim 1\%$ , but cause large  $T_c$  shifts of opposite signs. The magnetic behaviour of  $a\text{-Fe}_x\text{Zr}_{100-x}$  is dominated by the presence of exchange frustration [4], and  $T_c$  is therefore controlled by the balance between ferromagnetic (FM) and antiferromagnetic (AF) exchange. This balance will be affected both by the nearest-neighbour distances (which will in turn be modified by the dopant size) and also by the electron density in the alloy which can influence the FM–AF cross-over distance [6,7]. These complexities make a detailed accounting for the observed  $T_c$  shifts beyond the scope of the current work.

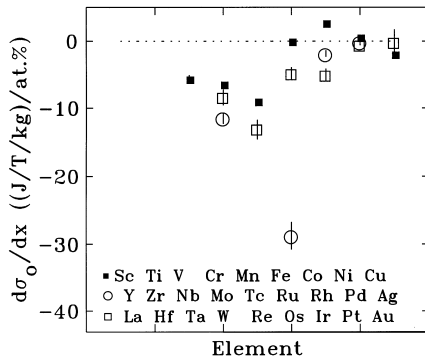


Fig. 3. The rate of change of the magnetisation,  $\sigma_0$ , at 5 K for  $a\text{-Fe}_{90-x}\text{TM}_x\text{Zr}_{10}$  alloys, where TM is a 3d, 4d or 5d transition metal.

The alloy magnetisation (Fig. 3) generally falls on doping, in part because the iron is being replaced by a nonmagnetic element. Most of the dopants are also heavier than Fe, giving a further contribution to the decline in mass-normalised magnetisation. There will also be a contribution from moments induced on the impurity. Orientational trends are the same for all three series: elements to the left of Fe have their moments oriented anti-parallel to the Fe moments, while for elements to the right, they tend to be parallel. For the 4d and 5d elements, these moments are generally small ( $\sim 0.1 \mu_B$ ) [27]. However, the situation for the 3d elements is more complex, as the moments are generally larger ( $\sim 1 \mu_B$ ), and the reported values exhibit substantial variations [28]. Fortunately, the alloys studied here are 90% iron and the impurity levels are low, so that the possible presence or absence of impurity moments has very little effect on the bulk magnetisation. They will be assumed to be absent in the analysis that follows. As with  $T_c$ , the basic pattern is simple. Elements to the left of Fe lead to substantial losses, while those to the right have a lesser effect. Again, Ru stands out as causing a much larger effect, in this case more than a factor of two larger than for any other element.

There are two ways in which a dopant can actively reduce the magnetisation (as opposed to passive effects of dilution and increasing the average atomic weight) these are (i) to reduce the Fe moment, and (ii) to introduce exchange frustration and

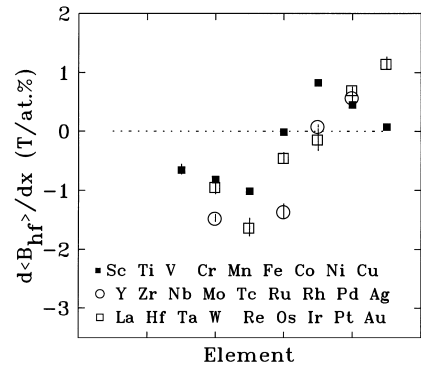


Fig. 4. The rate of change of the average hyperfine field,  $\langle B_{\text{hf}} \rangle$ , at 12 K for  $a\text{-Fe}_{90-x}\text{TM}_x\text{Zr}_{10}$  alloys, where TM is a 3d, 4d or 5d transition metal.

drive the magnetic structure non-collinear. We turn to the average hyperfine field  $\langle B_{\text{hf}} \rangle$  at the  $^{57}\text{Fe}$  nucleus determined by Mössbauer spectroscopy as a measure of the local Fe moment that is independent of the magnetic structure. Fig. 4 shows that the dopant effects on  $\langle B_{\text{hf}} \rangle$  measured at 12 K follow much the same pattern as  $\delta$ : elements to the left of Fe reduce  $\langle B_{\text{hf}} \rangle$ , while those to the right, increase it. This suggests that electron transfer may play some role in the moment changes. Comparison of Figs. 3 and 4 shows that the magnetisation and  $\langle B_{\text{hf}} \rangle$  are highly correlated, suggesting that in most cases, the magnetic structure changes little upon doping. There are some minor differences, in that Pt and Au show a significant increase in  $\langle B_{\text{hf}} \rangle$  but no change in  $\sigma$ , however this simply reflects the effect of the large atomic weights of these two elements on  $\sigma$ . Perhaps more striking is that Ru appears to be typical of the column in which it occurs in Fig. 4, and  $\langle B_{\text{hf}} \rangle$  does not show the same rapid reduction as  $\sigma$ . We have examined the magnetic effects of Ru [17,18] and Re [29] in some detail as these two dopants cause the most rapid reductions in  $T_c$  and  $\sigma$ . In both cases we observed a destruction of long-ranged magnetic order beyond a critical concentration of 2.5 at% and 4.5 at% for Ru and Re respectively. The loss of magnetisation caused by Ru, and to a lesser extent Re, is not the result of moment reduction, but rather an exchange frustration driven loss of collinear order.

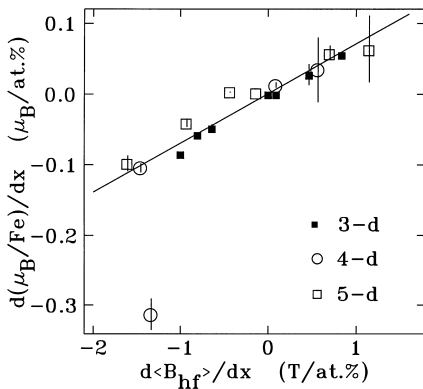


Fig. 5. Comparison of  $d\langle B_{\text{hf}} \rangle / dx$  and  $d\mu_{\text{Fe}} / dx$  for  $\text{Fe}_{90-x}\text{TM}_x\text{Zr}_{10}$  alloys showing the simple correlation between changes in the moment and the magnetisation for the majority of the alloys studied here. The one dropped point is due to Ru, and this plot serves to emphasise the anomalous effects of Ru-doping on the magnetic behaviour of this system.

The remarkable effects of Ru-doping can be emphasised by plotting the change in the iron moment (to normalise out contributions from dopants of differing atomic weights) against the change in  $\langle B_{\text{hf}} \rangle$  in Fig. 5. In preparing this figure, the impurity moments were assumed to be zero. Even if an impurity carried a moment of  $1 \mu_{\text{B}}$ , ignoring its contribution to  $\sigma_0$  only leads to an error in  $d(\mu_{\text{B}}/\text{Fe})/dx$  of  $\sim 0.01 \mu_{\text{B}}/\text{at}\%$ , less than most of the error bars in Fig. 5. All of the data from the various dopants collapse on to a single line, except for Ru. A linear fit to the rest of the data yields  $d\langle B_{\text{hf}} \rangle / d\mu_{\text{Fe}} = 14.3 \pm 0.8 \text{ T}/\mu_{\text{B}}$ . A value that is consistent with that found in  $\alpha\text{-Fe}$  ( $15 \text{ T}/\mu_{\text{B}}$ ) and also with the result deduced from a range of crystalline Y-Fe alloys ( $14.7 \text{ T}/\mu_{\text{B}}$ ) [30], confirming the remarkably wide applicability of this simple conversion factor to amorphous and crystalline Fe-based alloys. The departure of the Ru-doped alloys from the fitted line in Fig. 5 allows us to distinguish two influences on the magnetisation reduction caused by Ru. The change in  $\langle B_{\text{hf}} \rangle$  indicates that approximately one-third of the loss in  $\sigma_0$  can be accounted for through moment reduction, while the remaining two-thirds must be due to the rapid development of non-collinearity caused by exchange frustration.

## Acknowledgements

This work was supported by grants from: the Natural Sciences and Engineering Research Council of Canada, Fonds pour la formation de chercheurs et l'aide à la recherche, Québec, the Australian Research Council and The University of New South Wales.

## References

- [1] E. Batalla, Z. Altounian, J.O. Ström-Olsen, Phys. Rev. B 31 (1985) 577.
- [2] A.LeR. Dawson, D.H. Ryan, D.V. Baxter, Phys. Rev. B 54 (1996) 12238.
- [3] D.H. Ryan, J.M.D. Coey, E. Batalla, Z. Altounian, J.O. Ström-Olsen, Phys. Rev. B 35 (1987) 8630.
- [4] H. Ren, D.H. Ryan, Phys. Rev. B 51 (1995) 15885.
- [5] J.R. Thomson, Hong Guo, D.H. Ryan, M.J. Zuckermann, M. Grant, Phys. Rev. B 45 (1992) 3129.
- [6] R.F. Sabiryanov, S.K. Bose, O.N. Mryasov, Phys. Rev. B 51 (1995) 8958.
- [7] R.F. Sabiryanov, S.S. Jaswal, Phys. Rev. B 57 (1998) 7767.
- [8] D.H. Ryan, J.O. Ström-Olsen, W.B. Muir, J.M. Cadogan, J.M.D. Coey, Phys. Rev. B 40 (1989) 11208.
- [9] B.-G. Shen, Y.-Z. Wang, J.-C. Chen, J.-G. Zhao, W.-S. Zhan, J. de Phys. 49 (1988) C8–1161.
- [10] G.K. Nicolaides, G.C. Hadjipanayis, K.V. Rao, Phys. Rev. B 48 (1983) 12759.
- [11] P. Deppe, K. Fukamichi, M. Rosenberg, M. Sostarich, IEEE Trans. Magn. 20 (1984) 1367.
- [12] S.N. Kaul, P.D. Babu, Phys. Rev. B 45 (1992) 295.
- [13] K. Shirakawa, T. Kaneko, M. Nose, S. Ohnuma, H. Fujimori, T. Masumoto, J. Appl. Phys. 52 (1981) 1829.
- [14] J.A. Fernandez-Baca, J.W. Lynn, J.J. Rhyne, G.E. Fish, J. Appl. Phys. 61 (1987) 3406.
- [15] P.L. Paulose, V. Nagarajan, R. Nagarajan, R. Vijayaraghavan, Solid State Commun. 61 (1987) 151.
- [16] V. Nagarajan, P.L. Paulose, R. Vijayaraghavan, J. de Phys. 49 (1988) C8–1135.
- [17] D.H. Ryan, J.M. Cadogan, Zin Tun, J. Appl. Phys. 81 (1997) 4407.
- [18] D.H. Ryan, Zin Tun, J.M. Cadogan, J. Magn. Magn. Mater. 177–81 (1998) 57.
- [19] K. Shirakawa, S. Ohnuma, M. Nose, T. Masumoto, IEEE Trans. Magn. 16 (1980) 910.
- [20] T. Kaneko, K. Shirakawa, S. Abe, T. Masumoto, J. Magn. Magn. Mater. 54 (7) (1986) 305.
- [21] Z. Altounian, E. Batalla, J.O. Ström-Olsen, J. Appl. Phys. 59 (1986) 2364.
- [22] B. Window, J. Phys. E 4 (1971) 401.
- [23] M. Dikeakos, Z. Altounian, D.H. Ryan, S.J. Kwon, J. Non-cryst. Solids 250–252 (1999) 637.

- [24] G.K. Shenoy, F.E. Wagner (Eds.), Mössbauer Isomer Shifts, North-Holland, Amsterdam, 1978.
- [25] I. Vincze, I.A. Campbell, J. Phys. F 3 (1973) 647.
- [26] H. Akai, S. Blügel, R. Zeller, P.H. Dederichs, Phys. Rev. Lett. 56 (1986) 2407.
- [27] M.F. Collins, G.G. Low, Proc. Phys. Soc. 86 (1965) 535.
- [28] V.I. Anisimov, V.P. Antropov, A.I. Liechtenstein, V.A. Gubanov, A.V. Postnikov, Phys. Rev. B 37 (1988) 5589.
- [29] D.H. Ryan, Zin Tun, J.M. Cadogan, J. Appl. Phys. 85 (1999) 4506.
- [30] P.C.M. Gubbens, J.H.F. van Apeldoorn, A.M. van der Kraan, K.H.J. Buschow, J. Phys. F 4 (1974) 921.